

Magnetic phase diagram and structure of the magnetic phases in the quasi-one-dimensional antiferromagnet $\text{BaCu}_2\text{Si}_2\text{O}_7$: symmetry analysis.

V. Glazkov

*P.L.Kapitza Institute for Physical Problems, 117334 Moscow, Russia**

H.-A. Krug von Nidda

Experimentalphysik V, EKM, Institut für Physik,

Universität Augsburg, 86135 Augsburg, Germany

(Dated: February 7, 2020)

We have performed a symmetry analysis of the properties of the recently discovered quasi-one-dimensional compound $\text{BaCu}_2\text{Si}_2\text{O}_7$. The existence of the unusual spin-reorientation transitions is explained as an effect of the unusually strong relativistic interactions. The possible connection between the magnitude of the relativistic interactions and the low-dimensional structure of the $\text{BaCu}_2\text{Si}_2\text{O}_7$ is discussed. The structure of the magnetic phases is determined.

PACS numbers: 75.50.Ee, 75.30.Kz

Keywords: one-dimensional magnets, spin-reorientation transitions

I. INTRODUCTION.

Low-dimensional magnets are subject of intense interest due to the important role of the quantum fluctuations in these systems. As it was rigorously shown¹, no antiferromagnetic order can exist in an one-dimensional system. However, a weak interchain interaction leads to the formation of long-range magnetic order.

Different types of magnetic order (differing by the relative orientation of the spins) are possible if the unit cell of an antiferromagnet contains more than two magnetic ions. A transition from the paramagnetic phase to the phase with lowest exchange energy occurs at the Néel point. The difference between energies of different types of magnetic order in usual 3D-antiferromagnets is of the scale of the exchange interaction J .

Quasi-one-dimensional antiferromagnets have some unique properties: First, if the order types differ only by the orientations of the spins in the directions perpendicular to the chain, the energy difference between these ordered states will be small (of the scale of the small interchain-exchange interaction J_{\perp}). A second peculiarity arises from the microscopic structure of low-dimensional magnets. Small values of the interchain-exchange constants in inorganic compounds are frequently due to the orthogonality of the corresponding electron orbitals. Since this "90°"-rule is not applicable to other interchain interactions, relativistic interchain interactions (such as anisotropic or Dzyaloshinskii-Moriya exchange interactions) can compete with the interchain Heisenberg-exchange interaction. These features of low-dimensional magnets can result in magnetic phase transitions with a change of the exchange structure, as in the case of La_2CuO_4 .²

The recently discovered compound $\text{BaCu}_2\text{Si}_2\text{O}_7$ has attracted attention, since it was reported that it is a quasi-one-dimensional antiferromagnet³. The CuO_4 plaquettes form zigzag chains along the c direction of the orthorhombic crystal with a Cu-O-Cu bond angle of

about 124°. The exchange constants determined by means of neutron scattering⁴ are $J_c = 24.1$ meV, $J_b = 0.20$ meV, $J_a = -0.46$ meV and $J_{[110]} = 0.15$ meV. The susceptibility³ $\chi(T)$ also demonstrates a broad maximum characteristic for one-dimensional antiferromagnets⁵ at a temperature near 200 K.

The weak interchain interaction leads to the formation of long-range antiferromagnetic order at $T_N = 9.2$ K. The Néel temperature is well marked by a kink in χ_c , indicating easy-axis ordering in low magnetic field. Above T_N the susceptibility demonstrates a deviation from the Bonner-Fisher law³ — χ_c strongly increases on approaching the Néel temperature. The magnetic moment per Cu-ion is strongly reduced in the ordered phase due to the effect of quantum fluctuations: according to the inelastic neutron scattering experiments⁸ $\langle \mu \rangle = 0.15 \mu_B$.

Unexpectedly, the magnetization study in the ordered state reveals the existence of two spin-reorientation transitions at $\mathbf{H} \parallel c$ (transition fields $H_{c1} = 2.0$ T and $H_{c2} = 4.9$ T).⁶ Two spin-reorientation transitions are a surprising feature for a supposed-to-be-collinear antiferromagnet. Usually an easy-axis antiferromagnet exhibits only one spin-reorientation transition (spin-flop transition) caused by the competition of the gain in magnetization energy with the loss in anisotropy energy. The observation of an additional spin-reorientation transition⁷ at $H \perp c$ at the field $H_{c3} = 7.7$ T is also intriguing — the 'classical' easy-axis antiferromagnet does not undergo a spin-reorientation transition, if the external field is applied perpendicular to the easy axis of the anisotropy. Neutron-scattering experiments⁸ have shown that the intermediate-field phase is noncollinear. However, the origin of these exotic spin-reorientation transitions remains a mystery.

In the present paper we perform an analysis of the phase diagram and magnetic structure of $\text{BaCu}_2\text{Si}_2\text{O}_7$ from a macroscopic approach taking into account the symmetry of the crystal. We show that both two spin-reorientation transitions and the behavior of the suscepti-

TABLE I: Ferromagnetic and antiferromagnetic vectors allowed by the symmetry group D_{2h}^{16} .

$$\begin{aligned}
 \mathbf{M} &= \mathbf{S}_1 + \mathbf{S}_2 + \mathbf{S}_3 + \mathbf{S}_4 + \mathbf{S}_5 + \mathbf{S}_6 + \mathbf{S}_7 + \mathbf{S}_8 \\
 \mathbf{L}_1 &= \mathbf{S}_1 - \mathbf{S}_2 - \mathbf{S}_3 + \mathbf{S}_4 + \mathbf{S}_5 - \mathbf{S}_6 - \mathbf{S}_7 + \mathbf{S}_8 \\
 \mathbf{L}_2 &= \mathbf{S}_1 - \mathbf{S}_2 + \mathbf{S}_3 - \mathbf{S}_4 + \mathbf{S}_5 - \mathbf{S}_6 + \mathbf{S}_7 - \mathbf{S}_8 \\
 \mathbf{L}_3 &= \mathbf{S}_1 + \mathbf{S}_2 - \mathbf{S}_3 - \mathbf{S}_4 + \mathbf{S}_5 + \mathbf{S}_6 - \mathbf{S}_7 - \mathbf{S}_8 \\
 \mathbf{L}_4 &= \mathbf{S}_1 - \mathbf{S}_2 - \mathbf{S}_3 + \mathbf{S}_4 - \mathbf{S}_5 + \mathbf{S}_6 + \mathbf{S}_7 - \mathbf{S}_8 \\
 \mathbf{L}_5 &= \mathbf{S}_1 + \mathbf{S}_2 - \mathbf{S}_3 - \mathbf{S}_4 - \mathbf{S}_5 - \mathbf{S}_6 + \mathbf{S}_7 + \mathbf{S}_8 \\
 \mathbf{L}_6 &= \mathbf{S}_1 - \mathbf{S}_2 + \mathbf{S}_3 - \mathbf{S}_4 - \mathbf{S}_5 + \mathbf{S}_6 - \mathbf{S}_7 + \mathbf{S}_8 \\
 \mathbf{L}_7 &= \mathbf{S}_1 + \mathbf{S}_2 + \mathbf{S}_3 + \mathbf{S}_4 - \mathbf{S}_5 - \mathbf{S}_6 - \mathbf{S}_7 - \mathbf{S}_8
 \end{aligned}$$

TABLE II: Magnetic vector components transforming within the same representation. The signs in the first column show the effect of the symmetry operations I ($(x, y, z) \rightarrow (-x, -y, -z)$), C_z^2 ($(x, y, z) \rightarrow (\frac{1}{2} - x, -y, \frac{1}{2} + z)$) and C_y^2 ($(x, y, z) \rightarrow (-x, \frac{1}{2} + y, -z)$), correspondingly.

+++	L_1^x	L_2^y	L_3^z
++-	L_2^x	L_1^y	M^z
+--	L_3^x	M^y	L_1^z
-++	L_4^x	L_6^y	L_5^z
--+	L_5^x	L_7^y	L_4^z
-+-	L_6^x	L_4^y	L_7^z
---	M^x	L_3^y	L_2^z
---	L_7^x	L_5^y	L_6^z

bility above T_N are due to the unusually large relativistic terms in the thermodynamic potential.

II. CRYSTALLOGRAPHIC STRUCTURE AND MAGNETIC VECTORS.

The compound $\text{BaCu}_2\text{Si}_2\text{O}_7$ crystallizes in the space group $Pnma$ (D_{2h}^{16}) with four formula units per unit cell i.e. with 8 Cu^{2+} ions per unit cell. The magnetic ions occupy the $8d$ positions forming 4 zigzag chains along the c axis (see Figure 1). The lattice parameters are $a = 6.862 \text{ \AA}$, $b = 13.178 \text{ \AA}$, and $c = 6.897 \text{ \AA}$.

As it follows from neutron scattering, the magnetic unit cell coincides with the crystallographic one. In the ordered state each magnetic ion has a non-zero average

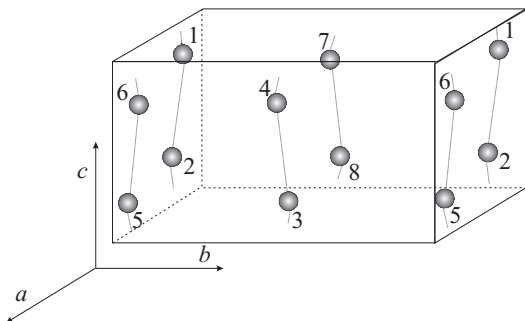


FIG. 1: Position of the magnetic ions in the unit cell.

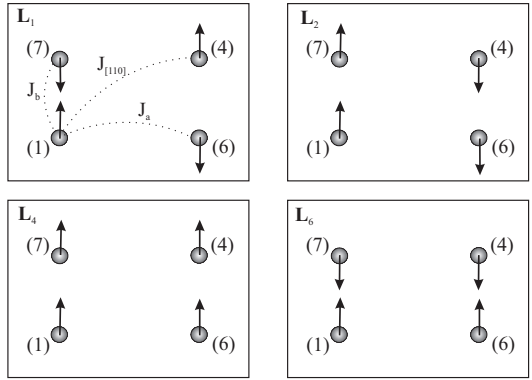


FIG. 2: Relative ordering of spins in the plane perpendicular to the chains for different antiferromagnetic vectors. The next layer is aligned antiferromagnetically. All spins can be rotated simultaneously on an arbitrary angle, including out of plane.

spin \mathbf{S}_i ($i = 1 \dots 8$). We will describe the magnetic structure using linear combinations of these spin vectors which components transform by the irreducible representations of the crystal-symmetry group. The space group D_{2h} exhibits only one-dimensional irreducible representations. Thus, the magnetic vector components will remain the same or change their sign under symmetry operations.

In further analysis we will use the inversion I ($(x, y, z) \rightarrow (-x, -y, -z)$) and two sliding axes: C_z^2 ($(x, y, z) \rightarrow (\frac{1}{2} - x, -y, \frac{1}{2} + z)$) and C_y^2 ($(x, y, z) \rightarrow (-x, \frac{1}{2} + y, -z)$) as independent symmetry operations. The fractional cell coordinates of the Cu^{2+} ion (1) in Figure 1 are given by $(\frac{1}{4} - 0.028, 0.004, \frac{3}{4} + 0.044)$ (see Ref. 3).

After trivial calculations we obtain 8 magnetic vectors (see Table I). The components of the magnetic vectors that transform within the same representation are gathered in Table II. Here and further on we will use coordinates with $x \parallel a$, $y \parallel b$ and $z \parallel c$, respectively. All possible magnetic structures for this symmetry group (including canted ones) can be analyzed in terms of these vectors.

A strong in-chain exchange favors ordering of the types \mathbf{L}_1 , \mathbf{L}_2 , \mathbf{L}_4 , \mathbf{L}_6 . In these cases in-chain neighboring spins are antiparallel. We will not consider other antiferromagnetic vectors in the further analysis. The relative orientation of the spins is shown for these order types in Figure 2.

If we will neglect the interchain interactions, in classical ($S \gg 1$) approximation the exchange energy for these ordering types is the same, i.e. the antiferromagnetically ordered state is four times degenerated. Interchain interactions lift this degeneration. Taking into account the exchange-integral values found by neutron scattering, one can estimate the hierarchy of the energies of the collinear ordering described by each of these vectors in the classical approximation.

$$\epsilon_6 < \epsilon_4 < \epsilon_2 < \epsilon_1 \quad (1)$$

TABLE III: Parameters of the thermodynamic potential (see Eqn. 3) at 5K per gramm, calculated from the data of Refs. 3,6,7.

χ_{\parallel}	$(1.98 \pm 0.05) \cdot 10^{-6}$ emu/g
χ_{\perp}	$(3.53 \pm 0.03) \cdot 10^{-6}$ emu/g
a_1	(846 ± 60) erg/g
a_2	(565 ± 45) erg/g
B_1	$-(1.39 \pm 0.07) \cdot 10^{-7}$ emu/g
B_2	$(1.06 \pm 0.12) \cdot 10^{-7}$ emu/g
ξ_x	$-(1.30 \pm 0.36) \cdot 10^{-7}$ emu/g
ξ_z	$(1.10 \pm 0.04) \cdot 10^{-6}$ emu/g

Zheludev et al. have found the structure of the magnetic phases by means of neutron scattering (see Ref. 8). In terms of the above-defined magnetic vectors the results of this work can be expressed as follows: At low fields (phase I, $H < H_{c1}$) all spins are aligned collinearly with antiferromagnetic vector $\mathbf{L}_6 \parallel z$. For the high-field phase (phase III, $H > H_{c2}$) the magnetic structure was found to be described by the same ordering type \mathbf{L}_6 with the antiferromagnetic vector along the x axis. The intermediate-field phase (phase II, $H_{c1} < H < H_{c2}$) was identified as noncollinear antiferromagnetic structure described by two magnetic vectors $\mathbf{L}_6 \parallel y$ and $\mathbf{L}_2 \parallel x$.

The easy-axis magnetic ordering is in agreement with susceptibility measurements, which show a characteristic kink at T_N for χ_c . The order of type \mathbf{L}_6 is also expected from classical estimations (see Eqn. (1)). However, the identification of the noncollinear phase can be questioned. First, since nuclear Bragg reflections coincide with magnetic ones, the determination of magnetic reflection intensities initially involves a big relative error. As it was shown in Ref. 8, a fit of the experimental data with the collinear model $\mathbf{L}_6 \parallel y$ yields $\chi^2 = 2.8$, while for the proposed noncollinear structure $\chi^2 = 2.4$ was found. Second, from Table II one can see that L_2^x and L_6^y transform differently under symmetry operations. This means that canting towards L_2^x cannot be induced by the internal fields.

III. MAGNETIC PROPERTIES OF $\text{BaCu}_2\text{Si}_2\text{O}_7$.

The following discussion is organized as follows: in Section III A we will analyze the magnetic phase diagram of $\text{BaCu}_2\text{Si}_2\text{O}_7$. The structure of the magnetic phases and the possible reason of the big values of the relativistic constants in the thermodynamic-potential expansion will be discussed in Section III B. The behavior of the static susceptibility above the Néel point will be treated in Section III C.

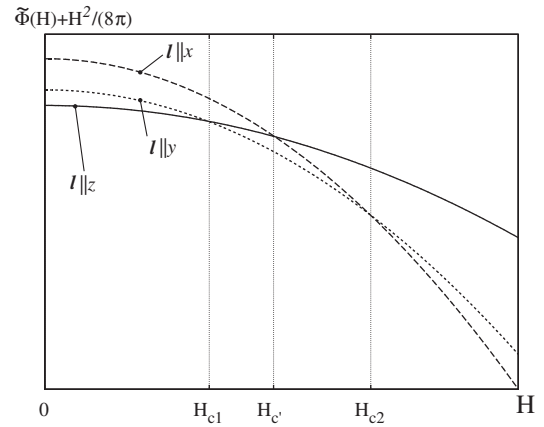


FIG. 3: Field dependences of the thermodynamic potential $\tilde{\Phi}$ for different orientations of the main antiferromagnetic vector. External field $\mathbf{H} \parallel z$.

A. Magnetic phase diagram.

The phase diagram of an antiferromagnet can be analyzed in terms of the main antiferromagnetic vector (i.e. \mathbf{L}_6) only.⁹ Distortions of the collinear order (i.e. canting of the sublattices) are of no interest in this subsection, while we are interested in the phase diagram only. Relativistic interactions leading to these distortions contribute to the corresponding relativistic constants, as it will be demonstrated in the next subsection.

Following the standard procedure, we will write down an expansion of the thermodynamic potential $\tilde{\Phi}(\mathbf{l})$, where $\mathbf{l} = \mathbf{L}_6/|\mathbf{L}_6|$.

The potential $\tilde{\Phi}$ is defined in such a way that¹⁰

$$\frac{\partial \tilde{\Phi}}{\partial H} = -\frac{B}{4\pi} = -M - \frac{H}{4\pi} \quad (2)$$

Since magnetization appears only in the presence of a magnetic field, the potential expansion can be written via the \mathbf{l} and \mathbf{H} variables.¹⁰ Requiring invariance of the energy to symmetry operations we obtain:

$$\begin{aligned} \tilde{\Phi}(\mathbf{l}, \mathbf{H}) = & a_1 l_x^2 + a_2 l_y^2 - \frac{\chi_{\parallel}}{2} (\mathbf{l} \cdot \mathbf{H})^2 - \\ & - \frac{\chi_{\perp}}{2} [\mathbf{l} \times \mathbf{H}]^2 + C_1 (\mathbf{l} \cdot \mathbf{H}) H_x l_x + \\ & + C_2 (\mathbf{l} \cdot \mathbf{H}) H_y l_y + B_1 l_x^2 H^2 + \\ & + B_2 l_y^2 H^2 - \frac{\xi_z}{2} H_z^2 - \frac{\xi_x}{2} H_x^2 - \frac{H^2}{8\pi} \end{aligned} \quad (3)$$

The small parameter in this expansion is the ratio between the relativistic constants and the exchange constants. The first two terms (a_i) describe the orthorhombic anisotropy, the terms containing χ_{\parallel} and χ_{\perp} describe the exchange part of the susceptibility — they do not change under simultaneous rotation of \mathbf{l} and \mathbf{H} on the same angle. The terms with ξ_{α} describe the relativistic

contribution to the susceptibility which is independent on the \mathbf{l} orientation. Of the higher order terms containing the magnetic field, we have kept only exchange-relativistic terms which are a product of exchange part (invariant under simultaneous rotation of \mathbf{l} and \mathbf{H}) and relativistic part. Other higher-order terms are smaller due to the supposed smallness of the relativistic constants and, thus, can be omitted. Easy-axis ordering at low fields requires that $a_1, a_2 > 0$.

Minimization over the orientations of \mathbf{l} in the exact orientations of the external magnetic field demonstrates that the antiferromagnetic vector \mathbf{l} is aligned along one of the crystallographic axes except maybe for the narrow field interval near the reorientation transitions where its behavior would be determined by the higher-order anisotropy terms.

The thermodynamic-potential expressions and magnetic susceptibilities for different possible orientations of \mathbf{H} and \mathbf{l} are given by:

$\mathbf{H} \parallel z$ (see Fig.3)

$$\mathbf{l} \parallel z : \quad \tilde{\Phi} = -\frac{\chi_{zz}^{(1)}}{2} H^2 - \frac{H^2}{8\pi} \quad (4)$$

$$\chi_{zz}^{(1)} = \chi_{\parallel} + \xi_z$$

$$\mathbf{l} \parallel y : \quad \tilde{\Phi} = a_2 - \frac{\chi_{zz}^{(2)}}{2} H^2 - \frac{H^2}{8\pi} \quad (5)$$

$$\chi_{zz}^{(2)} = \chi_{\perp} - 2B_2 + \xi_z$$

$$\mathbf{l} \parallel x : \quad \tilde{\Phi} = a_1 - \frac{\chi_{zz}^{(3)}}{2} H^2 - \frac{H^2}{8\pi} \quad (6)$$

$$\chi_{zz}^{(3)} = \chi_{\perp} - 2B_1 + \xi_z$$

$\mathbf{H} \parallel x$

$$\mathbf{l} \parallel z : \quad \tilde{\Phi} = -\frac{\chi_{xx}^{(1)}}{2} H^2 - \frac{H^2}{8\pi} \quad (7)$$

$$\chi_{xx}^{(1)} = \chi_{\perp} + \xi_x$$

$$\mathbf{l} \parallel y : \quad \tilde{\Phi} = a_2 - \frac{\chi_{xx}^{(2)}}{2} H^2 - \frac{H^2}{8\pi} \quad (8)$$

$$\chi_{xx}^{(2)} = \chi_{\perp} - 2B_2 + \xi_x$$

$\mathbf{H} \parallel y$

$$\mathbf{l} \parallel z : \quad \tilde{\Phi} = -\frac{\chi_{yy}^{(1)}}{2} H^2 - \frac{H^2}{8\pi} \quad (9)$$

$$\chi_{yy}^{(1)} = \chi_{\perp}$$

$$\mathbf{l} \parallel x : \quad \tilde{\Phi} = a_1 - \frac{\chi_{yy}^{(2)}}{2} H^2 - \frac{H^2}{8\pi} \quad (10)$$

$$\chi_{yy}^{(2)} = \chi_{\perp} - 2B_1$$

Now we can find the fields of the spin-reorientation transitions by equalizing the thermodynamic potentials in the phases with different orientations of \mathbf{l} .

$$\mathbf{H} \parallel z, (\mathbf{l} \parallel z \rightarrow \mathbf{l} \parallel y) : \quad H_{c1}^2 = -\frac{2a_2}{\chi_{\perp} - \chi_{\parallel} - 2B_2} \quad (11)$$

$$\mathbf{H} \parallel z, (\mathbf{l} \parallel y \rightarrow \mathbf{l} \parallel x) : \quad H_{c2}^2 = \frac{a_1 - a_2}{B_2 - B_1} \quad (12)$$

$$\mathbf{H} \parallel z, (\mathbf{l} \parallel z \rightarrow \mathbf{l} \parallel x) : \quad H_{c'}^2 = -2 \frac{2a_1}{\chi_{\perp} - \chi_{\parallel} - 2B_1} \quad (13)$$

$$\mathbf{H} \parallel y, (\mathbf{l} \parallel z \rightarrow \mathbf{l} \parallel x) : \quad H_{c3}^2 = -\frac{a_1}{B_1} \quad (14)$$

$$\mathbf{H} \parallel x, (\mathbf{l} \parallel z \rightarrow \mathbf{l} \parallel x) : \quad H_{c4}^2 = -\frac{a_2}{B_2} \quad (15)$$

All parameters involved can be estimated using the static magnetization data from Refs. 3,6 and the H_{c3} value from Ref. 7. Note, however, that the samples used in the above mentioned papers were different, thus, some uncertainty is possible. The values of the parameters calculated from the 5 K data are presented in Table III.

Since $a_1 > a_2$, the hard axis of the magnetization is established along the x direction. Substituting the found values to Eqn. 13, one can ascertain that $H_{c'} > H_{c1}$, i.e. a two-spin-reorientation transition scenario is more energy beneficial than a direct transition from $\mathbf{l} \parallel z$ to $\mathbf{l} \parallel x$. The positiveness of B_2 explains the absence of a phase transition for $\mathbf{H} \parallel x$: for $a_2 > 0$ and $B_2 > 0$ Eqn. 15 has no physical solutions.

The anisotropy constants determine the gaps of the antiferromagnetic resonance spectrum¹¹. Antiferromagnetic resonance on the BaCu₂Si₂O₇ was studied in Ref. 12 and two gaps given by $\Delta_1 = 40$ GHz and $\Delta_2 = 76$ GHz were found. The ratio of the AFMR gaps can be expressed as

$$\frac{\Delta_1}{\Delta_2} = \sqrt{\frac{a_2}{a_1}} \quad (16)$$

Inserting the values of the anisotropy constants from Table III yields for this ratio 0.57 ± 0.04 which is in perfect agreement with the value 0.53 found from the experiment. The absolute value of the AFMR gap can be approximated¹¹ as

$$\Delta_1 = \gamma \sqrt{2H_{a1}H_e} \sim 30 \text{ GHz} \quad (17)$$

which is in reasonable agreement with the experiment, since a good deal of uncertainty is involved in the estimation of the exchange field H_e in the case of a low-dimensional magnet. Thus, expansion (3) correctly describes the observed spin-reorientation transitions and is in agreement with other experimental observations.

The additional phase transitions occur as a result of the competition of anisotropy and relativistic corrections to the susceptibility. The transition at H_{c1} is a normal spin-flop transition: all spins are rotated perpendicular to the field direction and are aligned along the second-easy axis

y . At this transition the loss of the easy-axis anisotropy is compensated by the gain in magnetization energy, since $\chi_{\perp} > \chi_{\parallel}$. The second phase transition (at H_{c2}) is caused by the competition of the in-plane anisotropy and difference of the magnetization energy in different orientations of \mathbf{l} due to the relativistic corrections: The magnetic susceptibility for $\mathbf{l} \parallel x$ turns out to be larger than that for $\mathbf{l} \parallel y$, thus, the loss of anisotropy energy is overcome by the gain in magnetization energy. The spin-reorientation transition at $\mathbf{H} \parallel y$ is due to the same effect: relativistic corrections to the susceptibility make the susceptibility to be the largest for $\mathbf{l} \parallel x$, thus, the gain in magnetization energy overcomes the loss in anisotropy energy.

Note that the relativistic corrections B_i and ξ_{α} are unusually large in $\text{BaCu}_2\text{Si}_2\text{O}_7$: ξ_z turns out to be comparable with χ_{\perp} . The $B_i H^2$ terms normally should become comparable with the anisotropy constants only at magnetic fields of the scale of the exchange field. Thus, a mechanism, which strongly enhances the role of the relativistic interactions, has to be found. One possibility is the effect of anisotropic reduction of the spin in different phases. According to the neutron-scattering data⁸, the average magnetic moment of the Cu ion changes as \mathbf{l} changes its orientation. Accounting for this effect would result in the same exchange-relativistic terms in the thermodynamic-potential expansion. Another possible reason for the large values of these constants will be discussed in the next section.

It is necessary to recall that the above expansion of the thermodynamic potential was performed assuming the relativistic contributions to be small compared to the exchange part. Hence, higher-order terms have been neglected. However, in principle the increasing importance of the relativistic interactions should also lead to an increase of the higher-order terms, which especially would affect the phase transitions at higher fields (H_{c2} , H_{c3}). Moreover, this should give rise to other effects, such as a nonlinearity of the magnetization, which has not been reported yet. Nevertheless, the present experimental results can be consistently explained in the framework of our simplified approach. Therefore, it seems to be reasonable to start again with the assumption of small relativistic contributions in the following refinement of the thermodynamic potential with the aim to analyze the magnetic structure in detail.

B. Structure of the magnetic phases.

Relativistic interactions, such as the Dzyaloshinskii-Moriya interaction, can cause small distortions of the collinear structure, which can be expressed by magnetic vectors. These distortions, however, have to be compatible with the crystal symmetry. This means that the components of the magnetic vectors corresponding to the distortions in the given phase have to transform in the same way as the corresponding component of the main magnetic vector, i.e. they have to belong to the same rep-

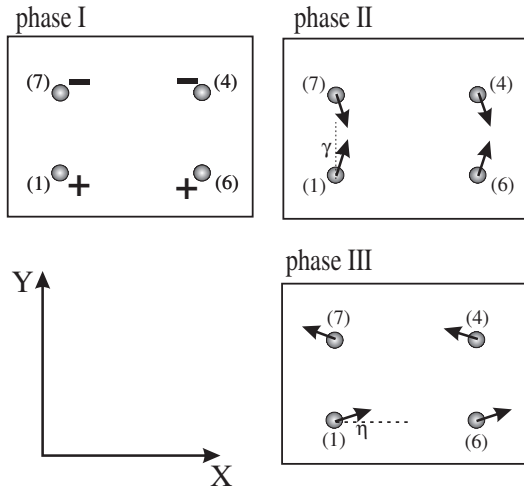


FIG. 4: Proposed structures for all phases (field-induced distortions are omitted): phase I: collinear structure l_6^z (direction of the spins is shown by the sign); phase II: weakly non-collinear antiferromagnet l_6^y and l_4^x ; phase III: weakly non-collinear structure l_6^x and l_4^y . Next layer of spins aligned antiferromagnetically.

resentation of the symmetry group. The possible types of canting of the spins can be easily found from Table II. We will consider here only distortions described by the magnetic vectors \mathbf{L}_1 , \mathbf{L}_2 and \mathbf{L}_4 , for only these magnetic vectors correspond to the antiferromagnetic in-chain order. Other distortions would lead to a violation of the in-chain antiferromagnetic ordering and, therefore, they are strongly suppressed by the strong in-chain exchange interaction.

Thus, we obtain

- phase I ($\mathbf{L}_6 \parallel z$)
no canting is allowed by symmetry
- phase II ($\mathbf{L}_6 \parallel y$)
 L_4^x is allowed
- phase III ($\mathbf{L}_6 \parallel x$)
 L_4^y is allowed

The structure of the magnetic phases is shown in Figure 4. Note that the proposed structure is different from that of Ref. 8, where canting described by the magnetic vector \mathbf{L}_2 was proposed. However, vector \mathbf{L}_2 has components transforming in the same way as the magnetization, i.e. distortions described by the components of \mathbf{L}_2 can be induced by the magnetic field.

To find the amplitudes of the distortions we have to write an expansion of the thermodynamic potential including vectors \mathbf{L}_1 , \mathbf{L}_2 and \mathbf{L}_4 and then to minimize this potential with respect to the components of these vectors. In this expansion we will normalize all magnetic vectors by the length of the main magnetic vector $|\mathbf{L}_6|$

$$\mathbf{l}_i = \mathbf{L}_i / |\mathbf{L}_6| \quad (18)$$

Requiring invariance of the energy to symmetry operations we obtain:

$$\begin{aligned}\tilde{\Phi} = & A_1 l_1^2 + A_2 l_2^2 + A_4 l_4^2 + \beta_1 l_6^x l_4^y + \beta_2 l_6^y l_4^x + \\ & + \alpha_1 l_1^y H^z + \alpha_2 l_2^x H^z + \alpha_3 l_2^z H^x + \alpha_4 l_1^z H^y + \\ & + \frac{\delta\chi}{2} l_4^2 H^2 - \frac{\chi'_\parallel}{2} (\mathbf{l}_6 \cdot \mathbf{H})^2 - \frac{\chi'_\perp}{2} [\mathbf{l}_6 \times \mathbf{H}]^2 + \\ & + a_1'(l_6^x)^2 + a_2'(l_6^y)^2 + B_1'(l_6^x)^2 H^2 + B_2'(l_6^y)^2 H^2 + \\ & + C_1'(\mathbf{l}_6 \cdot \mathbf{H}) H^x l_6^x + C_2'(\mathbf{l}_6 \cdot \mathbf{H}) H^y l_6^y - \\ & - \frac{\xi'_z}{2} H_z^2 - \frac{\xi'_x}{2} H_x^2 - \frac{H^2}{8\pi}\end{aligned}\quad (19)$$

We want to emphasize that this expansion is essentially the same as Eqn. (3). The only difference is that the interactions leading to the distortions of the collinear order are written explicitly, now.

In the expansion given above, the terms containing A_i are of exchange origin, they describe the loss in exchange energy. All of A_i are positive. The terms with β_i describe the canting of the antiferromagnetic sublattices (so called weak antiferromagnetism), those with α_i describe field-induced distortions. Both α_i and β_i parameters arise due to the microscopic Dzyaloshinskii-Moriya interaction.

Minimization over the components of magnetic vectors will demonstrate that the amplitudes of \mathbf{l}_1 , \mathbf{l}_2 and \mathbf{l}_4 are proportional to the ratio of some relativistic constant to the exchange constants A_i . We will suppose here that all relativistic constants are small compared with exchange constants. Then, the magnitude of \mathbf{l}_1 , \mathbf{l}_2 and \mathbf{l}_4 already contains relativistic smallness and we can neglect all higher-order relativistic terms containing these vectors.

Minimization of the (19) yields

$$l_1^y = -\frac{\alpha_1}{2A_1} H^z \quad (20)$$

$$l_1^z = -\frac{\alpha_4}{2A_1} H^y \quad (21)$$

$$l_2^x = -\frac{\alpha_2}{2A_2} H^z \quad (22)$$

$$l_2^z = -\frac{\alpha_3}{2A_2} H^x \quad (23)$$

$$l_4^x \approx \left(-\frac{\beta_2}{2A_4} + \frac{\beta_2}{4A_4^2} \delta\chi \cdot H^2\right) l_4^y \quad (24)$$

$$l_4^y \approx \left(-\frac{\beta_1}{2A_4} + \frac{\beta_1}{4A_4^2} \delta\chi \cdot H^2\right) l_4^x \quad (25)$$

The canting angles (see Figure 4) can be expressed as follows:

$$\gamma \approx \tan \gamma = l_4^x \quad \eta \approx \tan \eta = l_4^y \quad (26)$$

Note that the distortions of type l_2^x (which were found in Ref. 8) are possible, but they are induced by the external field and they are independent on the orientation of the main antiferromagnetic vector. Thus, they have to be

observed in all phases. Moreover, their amplitude should increase with increasing magnetic field, while according to the findings of Ref. 8 the noncollinearity is suppressed by the magnetic field in phase II.

On the other hand, the distortions described by the components of \mathbf{l}_4 are consistent with the experimental observations: they are absent in phase I, and their amplitude in phases II and III are governed by different constants β_i . The fact that the canting in phase III is much smaller than in phase II forces us to suppose that $\beta_1 \ll \beta_2$. A suppression of the canting in phase II corresponds to $\delta\chi > 0$.

Substituting these results to Eqn. 19 we obtain an equation of the same type as Eqn. 3 with renormalized constants. The comparison of Eqn. (3) with the results of the substitution yields

$$\chi_{\parallel, \perp} = \chi'_{\parallel, \perp} + \frac{\alpha_4^2}{2A_1} \quad (27)$$

$$\xi_z = \xi'_z + \frac{\alpha_1^2}{2A_1} + \frac{\alpha_2^2}{2A_2} - \frac{\alpha_4^2}{2A_1} \quad (28)$$

$$\xi_x = \xi'_x + \frac{\alpha_3^2}{2A_2} - \frac{\alpha_4^2}{2A_1} \quad (29)$$

$$a_1 = a'_1 - \frac{\beta_1^2}{4A_4} \quad (30)$$

$$a_2 = a'_2 - \frac{\beta_2^2}{4A_4} \quad (31)$$

$$B_1 = B'_1 + \frac{1}{8} \left(\frac{\beta_1}{A_4} \right)^2 \delta\chi \quad (32)$$

$$B_2 = B'_2 + \frac{1}{8} \left(\frac{\beta_2}{A_4} \right)^2 \delta\chi \quad (33)$$

If the relativistic constants are small compared to the exchange constants (as it was supposed in the expansion (19)), then the distortions caused by relativistic interactions result in small corrections to the constants connected with the main antiferromagnetic vector.

In the case of the low-dimensional antiferromagnet, it is another situation. The antiferromagnetic ordering of the types \mathbf{L}_1 , \mathbf{L}_2 , \mathbf{L}_4 , and \mathbf{L}_6 differs only by the relative orientation of the spins in the direction perpendicular to the chain. Thus, the loss in exchange energy for the canting from one of these order types to the other (i.e. A_i constants in the expansion (19)) is governed by the weak interchain exchange. As it was mentioned in the Introduction, in a quasi-one-dimensional magnet the interchain-exchange interaction can be comparable in strength with the relativistic interactions. Thus, the relativistic contributions in Eqns. 27-33 will not become small.

This argumentation cannot be considered as a strict proof of the role of low-dimensionality for the large values of the relativistic constants in Eqn. 3, because expansion (19) becomes incomplete, if some of the relativistic constants are comparable to the exchange ones.

However, the fact that in quasi-one-dimensional magnets strong distortions with small losses of exchange energy are possible, can result in an increase of the effect due to relativistic interactions.

C. Susceptibility of $\text{BaCu}_2\text{Si}_2\text{O}_7$ above the Néel point.

The susceptibility of $\text{BaCu}_2\text{Si}_2\text{O}_7$ above the Néel point strongly deviates from a Bonner-Fisher law⁵ characteristic for one-dimensional magnets^{3,6}. It demonstrates a broad maximum near 200 K but then shows a strong Curie-like increase to lower temperatures. This increase is anisotropic. It is strongest for χ_c and smallest for χ_a .

Such a behavior is typical for antiferromagnets with possible weak ferromagnetism^{13,14}. As it follows from Table II, weak ferromagnetism is allowed for antiferromagnetic order of types **L₁** and **L₂** — these vectors have components transforming in the same way as the magnetization components.

At the vicinity of the Néel point the amplitude of the order parameter is small and we can write down an expansion over the powers of the order parameter as in the usual Landau theory of second-order phase transitions:

$$\begin{aligned} \tilde{\Phi} = & A_1 L_1^2 + A_2 L_2^2 + A_4 L_4^2 + A_6 L_6^2 + \beta_2 L_6^y L_4^x + \\ & + \beta_1 L_6^x L_4^y + \alpha_1 L_1^y H^z + \alpha_2 L_2^x H^z + \alpha_3 L_2^z H^x + \\ & + \alpha_4 L_1^z H^y - \frac{1}{2} \chi_p H^2 - \frac{H^2}{8\pi} \end{aligned} \quad (34)$$

Here the A_i terms are of exchange origin, those with α and β are responsible for the canting, χ_p is the paramagnetic-state susceptibility. We neglect anisotropy terms and higher-order terms. Here we have used designations for the terms similar to those in Eqn. 19. Note, however, that coefficients with the same designations are different in Eqn. 19 and Eqn. 34.

At the transition point the factors A_i change their sign: it is positive above the transition temperature and negative below. In the vicinity of the corresponding Néel temperatures

$$A_i = \lambda_i (T - T_N^{(i)}), \quad \lambda > 0 \quad (35)$$

At the Néel point order of type **L₆** is established. We will suppose that in some temperature range above T_N the values of A_1 and A_2 continue to increase with increasing temperature and, thus, can be approximated as

$$A_{1,2} = A_{1,2}^{(0)} + \lambda'_{1,2} (T - T_N) \quad A_{1,2}^{(0)}, \lambda'_{1,2} > 0 \quad (36)$$

To find the values of the magnetic vector components we have to minimize expansion (34). Here we will restrict our analysis to the case of $T > T_N$. Above the Néel point we have $A_i > 0$, and in absence of an external field \mathbf{H} the minimum of the potential (34) corresponds to $|\mathbf{L}_i| = 0$. If a magnetic field is applied, weak antiferromagnetic order

parameters of the types **L₁** or **L₂** are induced. All other magnetic vectors are zero.

The existence of field-induced order parameters leads to an additional contribution to the susceptibility. Using Eqn. 36, we obtain for the magnetic susceptibilities:

$$\chi_{xx} = \chi_p + \frac{\alpha_3^2}{2(A_2^{(0)} + \lambda'_2(T - T_N))} \quad (37)$$

$$\chi_{yy} = \chi_p + \frac{\alpha_4^2}{2(A_1^{(0)} + \lambda'_1(T - T_N))} \quad (38)$$

$$\begin{aligned} \chi_{zz} = & \chi_p + \frac{\alpha_1^2}{2(A_1^{(0)} + \lambda'_1(T - T_N))} + \\ & + \frac{\alpha_2^2}{2(A_2^{(0)} + \lambda'_2(T - T_N))} \end{aligned} \quad (39)$$

I.e. with decreasing temperature the susceptibilities should increase. The amplitudes of this increase in different orientations³ allow to conclude that

$$\alpha_1^2 + \alpha_2^2 > \alpha_4^2 \gg \alpha_3^2 \quad (40)$$

The strongest effect for χ_{zz} is in accordance with the large relativistic contribution ξ_z in Eqn. 3.

IV. CONCLUSIONS

Starting from a symmetry approach we have analyzed the magnetic phase diagram and the corresponding magnetic structures of the antiferromagnet $\text{BaCu}_2\text{Si}_2\text{O}_7$. In the first step, we have obtained a thermodynamic potential in terms of the main antiferromagnetic vector only, demonstrating additional spin-reorientation transitions, which are due to the unusually strong relativistic terms in the expansion of the thermodynamic potential. The strength of the relativistic terms is probably connected to the low-dimensionality of the compound.

In the second step, we have refined the thermodynamic potential by including the magnetic vectors, which describe distortions of the magnetic structure compatible with the crystal symmetry. Based on our analysis, we proposed a structure of the magnetic phases (cf. Fig. 4), which is different from that in Ref. 8.

In addition, we were able to explain the deviations of the susceptibility from the Bonner-Fisher law on approaching the 3D-magnetic order. The analysis of the susceptibility behavior above T_N also shows the importance of the relativistic interactions for the understanding of the properties of $\text{BaCu}_2\text{Si}_2\text{O}_7$.

The strong enhancement of the relativistic effects should result in other interesting properties of this compound, such as nonlinear magnetization. Thus, further experimental and theoretical studies are necessary to achieve a deeper insight into the unusual properties of $\text{BaCu}_2\text{Si}_2\text{O}_7$.

Acknowledgments

This work was supported by the joint grant of the Russian Foundation for Basic Research and Deutsche

Forschungsgemeinschaft (DFG) No.01-02-004. The authors thank M.Zhitomirsky, A.I.Smirnov and S.S.Sosin for valuable discussions.

* Electronic address: glazkov@kapitza.ras.ru

¹ N. D. Mermin, H. Wagner, Phys. Rev. Lett. **17**, 1133 (1966).

² A. S. Borovik-Romanov, A. I. Buzdin, N. M. Kreines, S. S. Krotov, Sov. Phys. JETP Letters **47**, 697 (1988) [Pis'ma Zh.Exp.Teor.Fiz **47**, 600 (1988)].

³ I. Tsukada, Y. Sasago, K. Uchinokura *et al.*, Phys. Rev. B **60**, 6601 (1999).

⁴ M. Kenzelmann, A. Zheludev, S. Raymond *et al.*, Phys. Rev. B **64**, 054422 (2001).

⁵ Jill C. Bonner and Michael E. Fisher, Phys. Rev. **135**, A640 (1964).

⁶ I. Tsukada, J. Takeya, T. Masuda, and K. Uchinokura, Phys. Rev. Lett. **87**, 127203 (2001).

⁷ M. Poirier, M. Castonguay, A. Revcolevschi, and G. Dhaleine, Phys. Rev. B **66**, 054402 (2002).

⁸ A. Zheludev, E. Ressouche, I. Tsukada *et al.*, Phys. Rev. B **65**, 174416 (2002).

⁹ I. E. Dzyaloshinskii Sov. Phys. JETP **5**, 1259 (1957) [Zh.Exp.Teor.Fiz. **32**, 1547 (1957)].

¹⁰ L. Landau and I. Lifshitz, Theoretical Physics, vol. VIII.

¹¹ T. Nagamiya, K. Yosida and R. Kubo, Advances in Physics **4**(13), 1-112 (1955).

¹² R. Hayn, V. A. Pashchenko, A. Stepanov, cond-mat/0206151.

¹³ A. S. Borovik-Romanov, V. I. Ozhogin, Sov. Phys. JETP **12**, 18 (1961) [Zh.Exp.Teor.Fiz. **39**, 27 (1960)].

¹⁴ A. S. Borovik-Romanov, Lectures on low-temperature magnetism, Novosibirsk, 1976 (in Russian).